

Multiscale Computer Simulation of Tensile and Compressive Strain in Polymer-Coated Silica Aerogels.

Brian Good

Materials and Structures Division, NASA Glenn Research Center, Cleveland, Ohio.

ABSTRACT

While the low thermal conductivities of silica aerogels have made them of interest to the aerospace community as lightweight thermal insulation, the application of conformal polymer coatings to these gels increases their strength significantly, making them potentially useful as structural materials as well. In this work we perform multiscale computer simulations to investigate the tensile and compressive strain behavior of silica and polymer-coated silica aerogels.

Aerogels are made up of clusters of interconnected particles of amorphous silica of less than bulk density. We simulate gel nanostructure using a Diffusion Limited Cluster Aggregation (DLCA) procedure, which produces aggregates that exhibit fractal dimensions similar to those observed in real aerogels. We have previously found that model gels obtained via DLCA exhibited stress-strain curves characteristic of the experimentally observed brittle failure. However, the strain energetics near the expected point of failure were not consistent with such failure. This shortcoming may be due to the fact that the DLCA process produces model gels that are lacking in closed-loop substructures, compared with real gels. Our model gels therefore contain an excess of dangling strands, which tend to unravel under tensile strain, producing non-brittle failure. To address this problem, we have incorporated a modification to the DLCA algorithm that specifically produces closed loops in the model gels.

We obtain the strain energetics of interparticle connections via atomistic molecular statics, and abstract the collective energy of the atomic bonds into a Morse potential scaled to describe gel particle interactions. Polymer coatings are similarly described. We apply repeated small uniaxial strains to DLCA clusters, and allow relaxation of the center eighty percent of the cluster between strains. The simulations produce energetics and stress-strain curves for looped and nonlooped clusters, for a variety of densities and interaction parameters.

INTRODUCTION

Silica aerogels are low-density, highly porous materials possessing thermal properties that have made them of interest for a wide variety of applications [1-3]. Notably, the low thermal conductivities characteristic of such gels have led to the aerospace community's interest in these materials as lightweight thermal insulation. While these aerogels' fragility limits their utility in many applications, researchers in our laboratory have developed a method for monomer-coating aerogels and cross-linking the coatings, so as to greatly improve the gels' strength while not greatly impacting their insulating properties [4]. Such coated gels may prove suitable for use as lightweight structural

materials.

In order to provide an understanding of the mechanical behavior of the gels, and to provide predictive tools of use in their further development, we have constructed a multiscale model for the tensile and compressive failure of pristine and polymer-coated silica aerogels. The model is built on computer simulations using a modified diffusion-limited cluster aggregation (DLCA) scheme [5], along with a particle-based molecular statics procedure.

Earlier work using this model at times produced tensile failure behavior that was less brittle than what is experimentally observed. Visualization of these results suggests that there may be an unphysical uncoiling of the strands of secondary particles produced by the DLCA method, giving strain behavior more ductile than is observed experimentally. To correct this deficiency, we have added an additional step to the structural model generation process, in which strands having one free end are encouraged to attach themselves to the gel cluster that is the final result of the DLCA process, resulting in a more looped (and possibly more brittle) structure.

We perform a variety of multiscale computer simulations to investigate the tensile and compressive strain behavior of silica and polymer-coated silica aerogels. We discuss the strain behavior via energetics and stress-strain curves, for both tensile and compressive strain, for both looped and unlooped DLCA clusters.

STRUCTURAL MODEL

Experimentally, aerogels appear to consist of disordered aggregates of connected fractal clusters, with fractal behavior evident over a limited range of length scales [6-9]. In more detail, aerogels exhibit a low-density "pearl-necklace" structure that consists of tangled strands of approximately spherical particles. These "secondary" particles exhibit internal structure, consisting of smaller "primary" particles of amorphous silica of less than bulk density; an in-chain density of about 1.8 g/cm^3 has been reported by Woignier *et al.* [10]. Two examples of silica gels are shown in Figure 1.

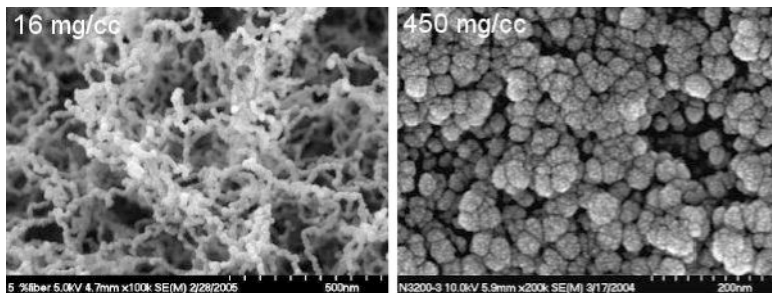


Figure 1. Silica Aerogels. 0.016 g/cm^3 (left), 0.450 g/cm^3 (right).

Model gel structures are produced using the Diffusion Limited Cluster Aggregation (DLCA) scheme. During aggregation, a computational cell is seeded with randomly-distributed secondary particles having a uniform radius of 15 nm. Particles are moved at random, forming subclusters, and, eventually, one large cluster. More specifically, a

particle or subcluster is chosen at random, with a probability given by $P_i = (m_i / m_0)^a$, where m_i and m_0 are the masses of the chosen subcluster and the lightest subcluster remaining in the computational cell, respectively, and a is a scaling parameter, here taken to be -0.5. The subcluster is moved in a random direction, and is then inspected for collisions with other particles or subclusters; if one or more collisions occur, the colliding subclusters and particles are merged into a single subcluster. Aggregation proceeds until only a single cluster remains.

In addition, to investigate the effects of looped structures in the DLCA clusters we have added a post-DLCA stage to cluster generation. All dangling strands are identified; each strand is traced from its end (a particle having a coordination of one) back to a "pivot point," a particle having coordination of three or greater. The "target" particle nearest to, but outside the strand is identified, and if possible the strand is rotated so as to allow the strand end to bond to the target particle, forming a loop. Because the looping process takes place after the DLCA process is complete, it is possible to compare the behavior of looped and unlooped versions of the same computational cell. We further assume that, in the case of polymer-coated gels, that the coatings bond conformally to the silica gel and do not significantly change the topology.

It should be noted that the looping process described above is different from the DLCA/Dangling Bond Deflection (DLCA-DEF) model of Ma *et al.* [11], in which loop formation takes place during the DLCA process.

MULTISCALE FAILURE MODEL

The clusters obtained from the structural model consist of spherical particles in contact. Micrographs suggest that real gel secondary particles are connected by interparticle "bridges" whose diameters are smaller than those of the connected particles. Polymer coatings are assumed to be of uniform thickness over particles and bridges, and failure is assumed to occur only through the bridges.

Gel failure simulations are performed using a multiscale technique, in which the strain energetics of the interparticle bridges and polymer coatings are described by simple potentials whose parameters are obtained from higher-fidelity atomistic simulations. A cylindrical atomistic bridge model of amorphous silica is given repeated small axial strains, with atomistic relaxation between strains accomplished via molecular statics. Atomistic interactions are computed using a Morse potential. The resulting energy-versus-strain curves are suggestive of the Universal Binding Energy Relation (UBER) of Rose, Smith and Ferrante [12], and we fit the bridge energy versus strain curve to a larger-scale interparticle Morse potential, as this form, with appropriate scaling, is known to accurately represent the UBER.

Strain energetics of the polymer coatings are treated in a similar manner. Because several polymer coatings are under development, we have chosen to use generic potential parameters for the Morse polymer potentials, characterizing them with respect to the

silica gel interparticle potential parameters.

RESULTS AND DISCUSSION

We have performed simulations for three densities of uncoated gels, and for coated gels derived from the same models, for a range of coating strengths, in both looped and unlooped states. We characterize the uncoated densities as low (0.029 g/cm^3), medium (0.067 g/cm^3) and high (0.184 g/cm^3). The silica interparticle potential well depth parameter V_0 is $2.5 \cdot 10^{-10}$ ergs and the well depths for the coatings are $1.0 \cdot 10^{-12}$ ergs (weak), $2.5 \cdot 10^{-10}$ ergs (medium) and $2.5 \cdot 10^{-9}$ ergs (strong). The coating thickness is assumed to be 0.1, normalized to the radius of the interparticle silica bridge. With secondary particle interactions described by the large-scale Morse potential as above, a tensile strain is applied to each DLCA cluster, using a molecular statics procedure, until the energy reaches a maximum (tensile strain) or shows an abrupt increase (compressive strain).

Representative plots of energy versus strain for tensile and compressive strain are shown in Figure 2. Energies are measured with respect to the energy of the corresponding relaxed but unstrained cell. The tensile energies exhibit qualitatively similar behavior—the curvature is positive at small strain, but become negative at larger strain. In previous work we have found that the energy under tensile strain reaches a broad maximum at larger strains. Compressive energies, on the other hand, show only positive curvature, with no indication of failure at the strains studied. It is known that, because of the high degree of porosity, aerogels under compression may exhibit densification before failure,

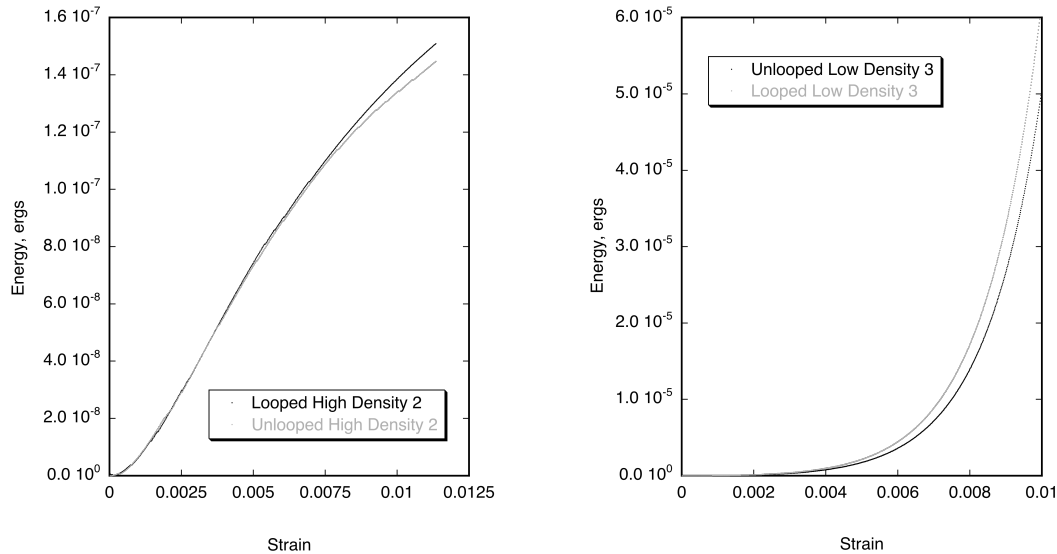


Figure 2. Tensile strain energetics, high density (a); Compressive strain energetics, low density (b).

and that is consistent with the energetics seen here, although experimentally the densification occurs over a broader range of compressive strain. It is evident that compressive failure occurs at a larger strain than is shown here. It should be noted that all plots shown use data taken from weak-polymer simulations. Because the forms of the silica and polymer interparticle potentials are similar, no qualitative differences are observed among simulations using different polymer potential strengths.

It is apparent that, while the looped version of a model gel cluster typically exhibits higher energy and stress at a given strain, the shapes of the energy and stress-strain curves for looped and unlooped cells are very similar. This suggests that adding a looping stage to model gel formation does not qualitatively change the failure mechanism. Ma *et al.* have found that when the looping process is carried out during the DLCA process, rather than afterward, model gel behavior is more brittle.

It can be seen that the variation in energy among different clusters having the same density but obtained from different randomized initial states of the computational cells before aggregation is comparable in magnitude to the difference between looped and unlooped versions of the same cell. However, it should be noted that in almost all cases, the looped cell exhibits a larger energy, and higher stress, at a given strain.

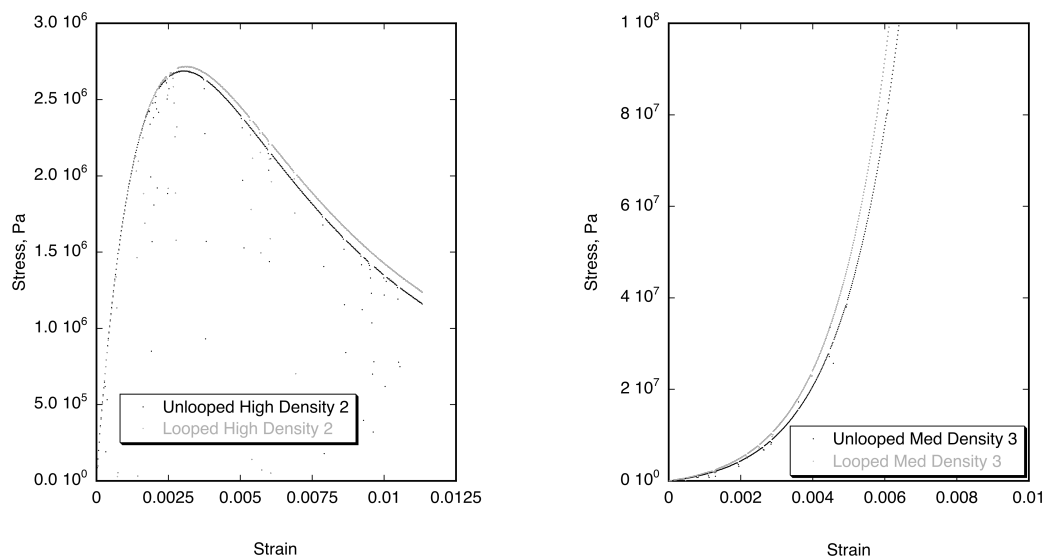


Figure 3. Stress versus strain. Tensile high density (a); Compressive medium density (b).

Stress-strain curves are shown in Figure 3. Under small tensile strain, the model gels exhibit behavior consistent with brittle failure; the stress increases sublinearly before reaching a maximum. There is no abrupt decrease in the stress indicative of sudden failure, but this may be attributed to uncoiling of the strands within the cluster. If we

define the point of failure as the strain at which maximum stress is reached, our values of maximum stress are consistent with the work of Meador *et al.* [13], who report failure in the range of a few MPa. Our strain at failure values, however, are approximately 0.3 percent, considerably smaller than typical experimental values of about a percent. As is the case with the energies, the stress at a given strain is slightly larger for the looped version of the cells than for the unlooped ones. Under compressive strain, the stress increases without exhibiting a maximum, consistent with densification below the strain at failure.

CONCLUSIONS

We have performed multiscale computer simulations of the tensile and compressive failure of polymer-coated silica aerogels. The simulations of gel structure were based on a diffusion-limited cluster aggregation procedure, including, in some cases, an additional looping stage. Strain energetics and stress-strain behavior were modeled using a molecular statics procedure. Simulations were carried out at densities representative of real aerogels. Tensile stress-strain curves exhibit characteristics suggestive of brittle failure. Model gel stresses are consistent with experiment, but the strain at failure is smaller than observed experimentally. Compressive strain produced behavior characteristic of densification, but no compressive failure at the strain values used in the simulations. Looped cells exhibit slightly larger energies and stresses than do the corresponding unlooped ones, but the energy and stress-strain curves are very similar in shape, indicating that adding loops to the DLCA clusters after cluster formation does not fundamentally change the behavior of the model.

REFERENCES

1. N. Husing and U. Schubert, *Angew. Chem. Int. Ed.* **37**, 22 (1998).
2. A. C. Pierre and G. M. Pajonk, *Chem. Rev.* 2002, **102**, 4243 (2002).
3. J. L. Rousset, A. Boukenter, B. Champagnon, J. Dumas, E. Duval, J. F. Quinson and J. Serughetti, *J. Phys.: Condens. Matter* **2**, 8445 (1990).
4. M. A. B. Meador, E. F. Fabrizio, F. Ilhan, A. Dass, G. Zhang, P. Vassilaras, J. C. Johnston and N. Leventis, *Chem. Mater.* **17**, 1085 (2005).
5. P. Meakin, *Phys. Rev. Lett.* **51**, 1119 (1983).
6. D. W. Schaeffer, J. E. Martin and K. D. Keefer, *Phys. Rev. Lett.* **56**, 2199 (1986).
7. T. Freltoft, J. K. Kjems and S. K. Sinha, *Phys. Rev. B* **33**, 269 (1986).
8. R. Vacher, T. Woignier, J. Pelous and E. Courtens, *Phys. Rev. B* **37**, 6500 (1988).
9. A. Hasmy, E. Anglaret, M. Foret, J. Pelous and R. Julien, *Phys. Rev. B* **50**, 1305 (1994).
10. Woignier : T. Woignier and J. Phalippou, *J. Non-Cryst. Solids* **93** 17 (1987).
11. H.-S. Ma, R. Jullien and G. W. Scherer, *Phys. Rev. E* **65**, 041403 (2002).
12. J. H. Rose, J. Ferrante and J. R. Smith, *Phys. Rev. Lett.* **47**, 675 (1981).
13. M.A.B. Meador, S. L. Vivod, L. McCorkle, D. Quade, R. M. Sullivan, L. J. Ghosn, N. Clark and L. A. Capadona, *J. Mater. Chem.* **18**, 1852 (2008).